Combination of Raman Microscopy, Multiwell Plate Experimental Designs, and BTEM Analysis for High-Throughput Experimentation

Effendi Widjaja, Chuanzhao Li, and Marc Garland*

Process Science and Modeling, Institute of Chemical and Engineering Sciences, Agency for Science, Technology and Research (ASTAR), 1 Pesek Road, Jurong Island, Singapore 627833

Received August 19, 2008

Both nonreactive and reactive multiwell plate experiments were combined with Raman microscopy and band-target entropy minimization (BTEM) analysis. The multicomponent nonreactive experiments showed that accurate pure component spectral estimation is possible without recourse to any spectral libraries. The multicomponent reactive experiments showed that, in addition to accurate pure component spectral estimation, concentration profiles can be obtained for quantitative purposes. In the present case, the solvent and time dependence of a cycloaddition reaction was addressed as the high-throughput experimentation issue. A total of 1152 experimental spectra were collected and analyzed. Two methods were used, namely, (A) each solvent set was individually analyzed and (B) the entire set of spectra, from 4 different solvents, were analyzed all together. Method B provided very satisfactory results. The present study with combined Raman-multiwell plate-BTEM analysis establishes proof of concept. The new approach appears to be applicable to other frequently conducted combinatorial/high-throughput experimentations. These include, but are not restricted to, chemo- and regioselective studies, solid-phase syntheses, etc.

Introduction

The use of robotics for experimentation and the prevalence of highly automated instrumentation has resulted in a dramatic increase in information, particular in the chemical sciences.[1−4] However, in many combinatorial and high-throughput experimental (HTE) situations, the analysis of data has lagged the experimental advances. This situation is particular true in the area of spectroscopic instrumentation applied to reaction analysis in the chemical sciences.[5−7]

In the present contribution, a very specific situation is addressed, namely, Raman microscopy measurements of multiwell plates. Raman spectroscopy is a widely used analytical tool with a very wide range of applications, involving gas, liquid, and solid samples.[8,9] Multiwell plates are becoming an increasingly chosen route for high-throughput experimentation.[10−12] This situation has arisen, in part, because of the small quantities of consumable materials needed, as well as the wide variety of instrumentation that can accommodate multiwell sampling.

Recently, a blind-source separation algorithm, band-target entropy minimization (BTEM), was developed for analyzing large sets of multicomponent spectroscopic measurements. This algorithm reconstructs the pure component spectra of the constituents without recourse to any a priori information, particularly spectral libraries. It has been applied to a wide range of spectroscopic measurements (FTIR,[13−15] Raman,[16,17] MS,[18] UV−vis,[19] CD,[19] NMR[20]) and can frequently recover the pure component spectra of trace constituents (i.e., at ppm concentrations or less).[21,22] Consequently, it has been primarily used for in situ spectroscopic studies of complex reactions, where dozens of constituents may be simultaneously present.[23] Clearly, the simultaneous analysis of thousands of reaction spectra and the subsequent reconstruction of all the observable constituents present is a very powerful tool that can help to clarify detailed chemistry quickly and aid in quantitative analysis.

In the following, Raman microscopy, multiwell plate experimentation, and BTEM analysis are combined (with various experimental designs), both in a nonreactive and a simple reactive context. The results clearly demonstrate that the entire spectroscopic data set from multiwell plates can be analyzed together to obtain the pure component spectra of the observable species and to obtain relative time-dependent concentration profiles. Proof of concept is established. This finding suggests that the present combinatorial and HTE approach should be applicable in the future to other related areas, such as chemo- and regioselective studies, solid-phase syntheses, etc.

Experimental Section

General. The chemicals, namely, the solvents cyclohexane (>99%), tetrahydrofuran or THF (>99%), acetone (>99.5%), toluene (>99.5%), *n*-heptane (>99%), dimethylformamide or DMF (>99.8%) and reactants 1,3-cyclohexadiene (>97%) and dimethyl ester acetylenedicarboxylic acid (>98%), were all used as received without further purification. All chemicals were purchased from Sigma-Aldrich.

A quartz glass 96-well plate with cover (Helma) was used in all experiments in conjunction with a Raman microscope (Renishaw InVia Reflex). The spectroscopic measurements were conducted with a near-infrared laser (785 nm) at 50%

* To whom correspondence should be addressed. Phone: +65- 6796-3947. Fax: +65- 6316-6185. E-mail: marc_garland@ices.a-star.edu.sg.

10.1021/cc800139x CCC: $40.75
Published on Web 02/04/2009

maximum power using a 5× objective. The automated routine "Microplate Mapping" within Wire 2.0 was used to acquire the Raman spectra. The scanning range for the spectra was set to 100−3600 cm^{-1} (Stokes) with an average resolution of slightly less than 1 cm^{-1}. This resulted in 4479 channels of data for each spectrum. Each stored spectrum was the result of one scan, no spectral coadditions were performed. Approximately 2.5 h was required for a single mapping of the 96-well plate. The Raman microscope was adjusted to focus into the liquid phase at $\sim^1/_2$ depth.

The nonreactive multiwell experiments were conducted with mixtures of cyclohexane, acetone, toluene, and tetrahydrofuran. Aliquots of 30, 60, 90, and 120 μL of each solvent were dispensed into each well, resulting in a total liquid volume of ~300 μL. The aliquots were distributed in such a way that the experimental design produced 16 distinct compositions in the plate (3 × 2 wells each). Since the total volume of a well is ~400 μL, there were ~100 μL of gas phase above each sample. Each cell was mechanically stirred briefly with a spatula before covering the multiwell plate with the thin quartz-glass top-plate. No sealing was used between the multiwell plate and the top-plate for this ~2.5 h Raman mapping. The multiwell plate was immediately loaded into the $x-y-z$ motorized stage of the microscope, and the mapping sequence was started. This experiment resulted in 96 Raman spectra for off-line analysis. The measurements were conducted at ~298 K in the absence of stirring.

The reactive experiments involved the cycloaddition of 1,3-cyclohexadiene to dimethyl ester acetylenedicarboxylic acid to give the product dimethyl bicyclo[2,2,2]octa-2,5-diene-2,3-dicarboxylate.[24,25] This reaction is highly selective and relatively slow (characteristic reaction times are days). Because the solvent dependence of this reaction was the main aim of the investigation, the 96-well plate was first partitioned into 4 regions (8 × 3 wells each) corresponding to the 4 solvents used, namely, cyclohexane, toluene, DMF, and *n*-heptane. A different set of solvents was chosen for the reactive experiments to further demonstrate the robustness of BTEM analysis (thus avoiding a repetition of the nonreactive results).

The solvent volume used in each cell was 150 μL. In each of the 4 partitions, the 1,3-cyclohexadiene was dispensed as either 30, 40, 60, or 80 μL aliquots, and the alkyne was dispensed in either 30, 35, or 40 μL aliquots. This resulted in 12 distinct initial composition regions (1 × 2 wells each) in each partition. Therefore, for the entire 96-well plate, 48 distinct compositions were present at the beginning of the experiment. A light coating of silicone vacuum grease was added to the top surface of the multiwell plate, and the quartz glass cover was placed on top. The use of a sealant was considered prudent for this multiple-day reactive Raman mapping. The 96-well plate was mapped a total of 12 times over a ~72 h period (see Table 1 for details). The measurements were conducted at ~298 K in the absence of stirring. This experiment resulted in 1152 (12 × 96) Raman spectra for off-line analysis.

Computational Details. The Raman spectra from the nonreactive and reactive experiments were first despiked to remove spectral artifacts caused by cosmic rays. The preprocessed spectra were then analyzed using a variety of chemometric techniques. The self-modeling curve resolution algorithm, band-target entropy minimization (BTEM), was the primary tool used. BTEM estimates the pure component spectra of constituents in multicomponent solutions without the need for any spectral libraries of other a priori information.

Table 1. Details Concerning the Mapping Numbers and Corresponding Reaction Times for Cycloaddition Reaction and the Raman Measurements

mapping number	day	reaction time for beginning of each 96-well Raman map
1	1	0 h 0 min
2	1	2 h 35 min
3	1	5 h 40 min
4	2	22 h 10 min
5	2	25 h 10 min
6	2	27 h 35 min
7	2	30 h 10 min
8	3	46 h 35 min
9	3	49 h 10 min
10	3	52 h 5 min
11	3	55 h 35 min
12	4	70 h 5 min

BTEM has been frequently used in conjunction with vibrational spectroscopies to analyze results from both organometallic and complex homogeneous catalyzed organic syntheses.[13,21−23] In such studies, where the chemical system may consist of 10−20 observable species, excellent signal-to-noise estimates are frequently obtained from species at the part per million or sub-part per million level.[21,22] The accuracy of these spectral estimates has been repeatedly demonstrated, in the above-mentioned studies, as well as in the chemometrics literature.[15] The computational details of BTEM have been thoroughly documented elsewhere and will not be repeated here.[14,15,23]

Subsequent modeling included a least-squares fit of the pure component spectra onto the individual experimental spectra taken from each well and, hence, the determination of the relative concentration profiles. In addition, with the proper type of experimental design, it is also possible to use the set of spectral estimates to obtain the properly scaled absorptivites/scattering coefficients as well and, hence, the real concentration profiles.[23]

Results

Nonreactive System. The set of 96 despiked Raman spectra are shown in Figure 1. These were subjected to BTEM analysis, and only four spectral patterns were found and reconstructed as shown in Figure 2. All four spectral estimates have good signal-to-noise ratios, and these spectral patterns correspond to the four solvents used, namely, cyclohexane, acetone, toluene, and tetrahydrofuran. Moreover, the inner product between these spectral estimates and the pure references were 0.9842, 0.9825, 0.9818, and 0.9858, respectively. In other words, the spectral estimates obtained from the multivariate analysis of the 96 mixtures and their corresponding pure references are very similar.

The four spectral estimates were then mapped back onto the original 96 despiked experimental Raman spectra. In general, the least-squares fit was quite good. Figure 3 shows

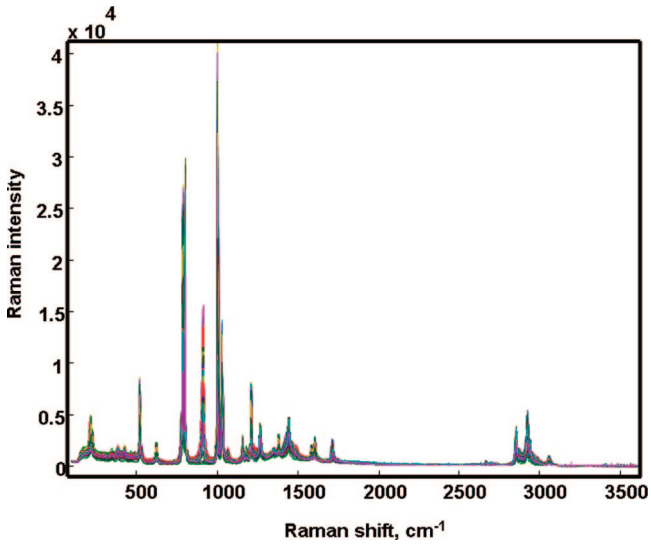

Figure 1. Despiked Raman spectra for a single 96-well nonreactive experiment involving four solvents in the experimental design.

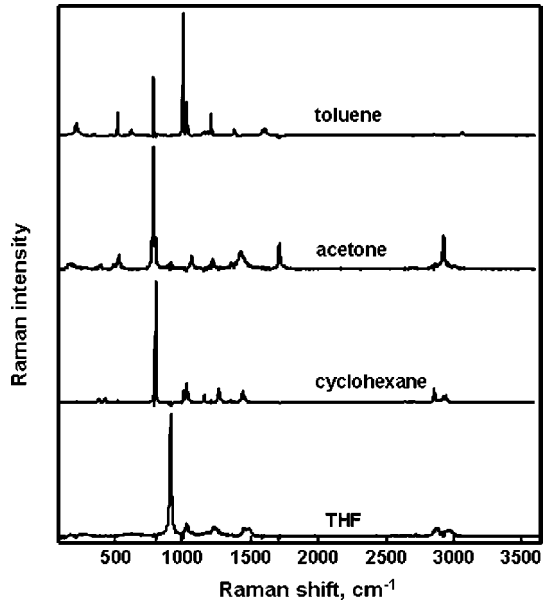

Figure 2. Pure component spectral estimates for cyclohexane, acetone, toluene, and tetrahydrofuran obtained from BTEM multivariate analysis of the 96-well plate nonreactive experiment.

an example of the despiked Raman spectrum from well no. 1 and the corresponding least-squares fit.

The analysis of the present nonreactive system indicates that full-length (100−3600 cm^{-1}) Raman spectral reconstruction is possible from a multicomponent multiwell plate experiment. In addition, the inner-product analysis and least-squares analysis suggests that the quality of the spectral reconstructions is sufficient for good quantitative results.

Reactive System. The set of 1152 despiked Raman spectra from the cycloaddition reaction were subjected to BTEM analysis in two different ways. In method A, the 288 spectra associated with each of the four solvents were analyzed separately. In method B, all 1152 despiked Raman spectra were analyzed together.

Figure 4 shows the spectral estimates for 1,3-cyclohexadiene obtained by analyzing the data according to method A (separate analyses for each solvent) and according to

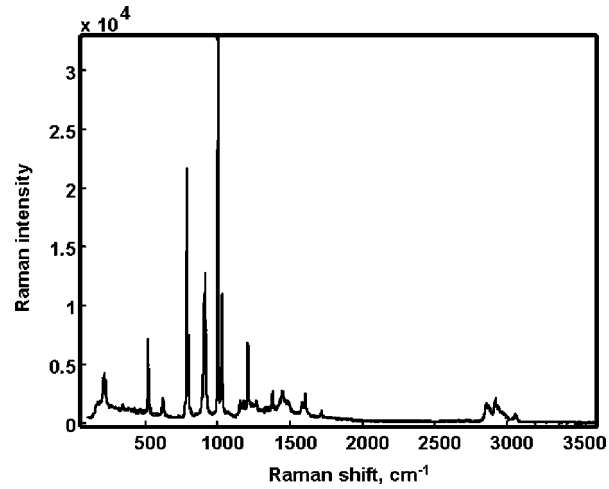

Figure 3. Despiked Raman spectrum from well no. 1 (solid line) and the least-squares fit (dashed line) using the four spectral estimates of cyclohexane, acetone, toluene, and tetrahydrofuran obtained from BTEM.

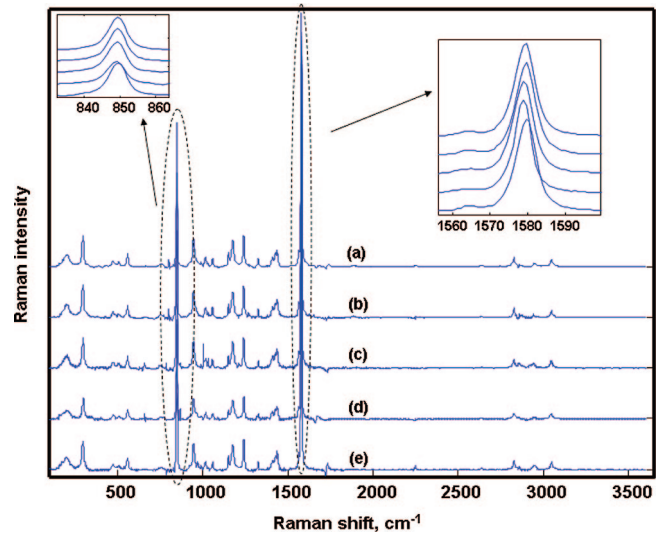

Figure 4. Comparison of the 1,3-cyclohexadiene spectral estimates obtained from method A and method B and expanded views of two regions with significant Raman scatter: (a) method B, (b) method A from cyclohexane, (c) method A from toluene, (d) method A from DMF, and (e) method A from *n*-heptane.

method B (combined analysis for all solvents). It can be seen that the spectral estimates for 1,3-cyclohexadiene obtained from each solvent system are quite similar, although not identical. Indeed, small shifts in the largest bands are clearly discernible. Furthermore, the spectral estimate for 1,3-cyclohexadiene obtained from all 1152 Raman spectra (method B) is similar to those obtained by method A. Close inspection shows that the bands in the spectral estimate from method B are in fact slightly broader than those obtained in the individual solvents. This result arises from the fact that the spectral estimate from all 1152 Raman spectra is a convolution of all the individual observations. The spectral estimate from method B also has a noticeably better signal-to-noise ratio because of the larger number of measurements performed.

A similar approach was taken for the spectral estimates of alkyne (Figure 5) and product (Figure 6). In general, similar types of results and conclusions were obtained.

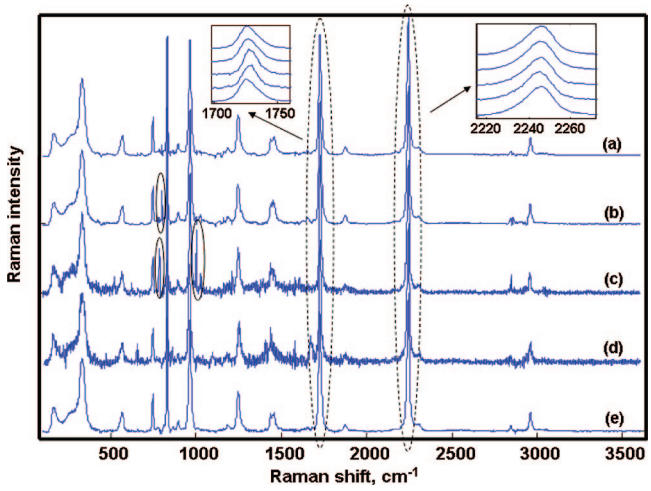

Figure 5. Comparison of the alkyne spectral estimates obtained from method A and method B. Note the improved signal-to-noise ratio obtained using method B. Circles indicate clear artifacts in the spectral estimates. (a) Method B, (b) method A from cyclohexane, (c) method A from toluene, (d) method A from DMF, and (e) method A from *n*-heptane.

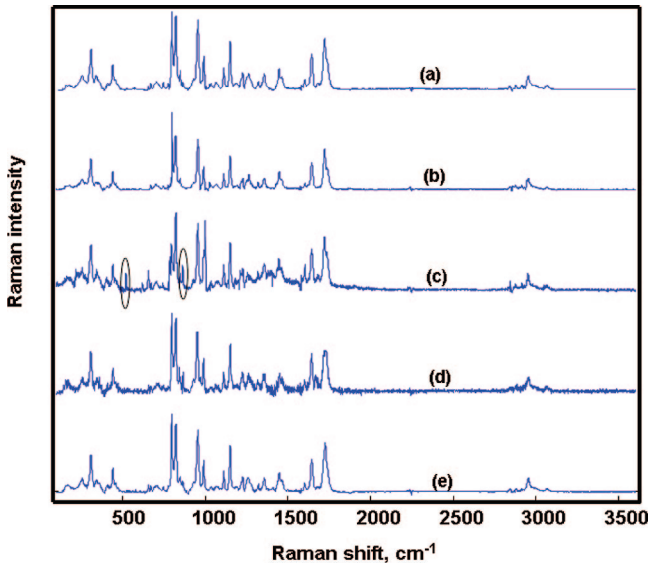

Figure 6. Comparison of the product spectral estimates obtained from method A and method B. Note the improved signal-to-noise ratio obtained using method B. Circles indicate clear artifacts in the spectral estimates. (a) Method B, (b) method A from cyclohexane, (c) method A from toluene, (d) method A from DMF, and (e) method A from *n*-heptane.

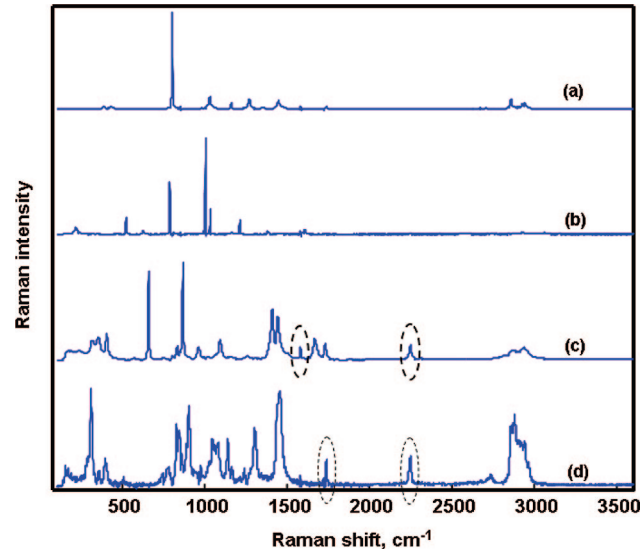

Figure 7. Spectral estimates of the four solvents using method A. Circles indicate clearly identifiable artifacts in the spectral reconstructions. (a) Cyclohexane, (b) toluene, (c) DMF, and (d) *n*-heptane.

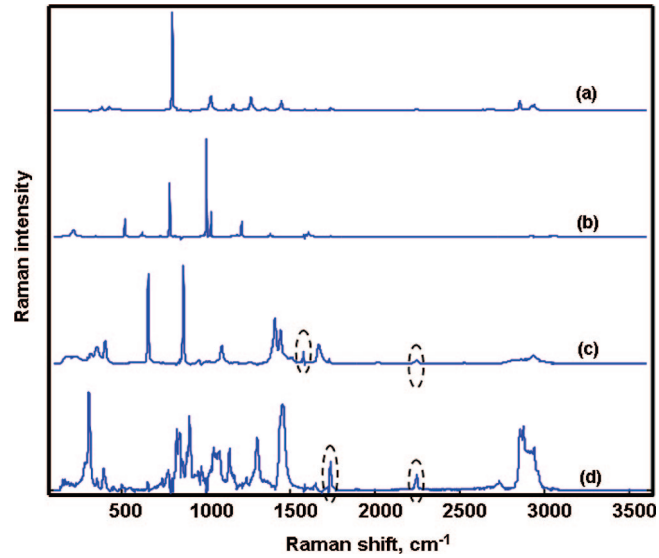

Figure 8. Spectral estimates of the four solvents using method B. Circles indicate clearly identifiable artifacts in the spectral reconstructions. Note the improved signal-to-noise of the estimates compared to Figure 7. (a) Cyclohexane, (b) toluene, (c) DMF, and (d) *n*-heptane.

Specifically, the spectral estimates for (i) alkyne and (ii) product obtained from each solvent system are quite similar, although not identical. Small shifts in the largest bands are again clearly discernible. In addition, the spectral estimates for (i) alkyne and (ii) product obtained from all 1152 Raman spectra (method B) are similar to but better than (signal-to-noise ratio) those obtained by method A.

Spectral estimates of the solvents were also obtained, by both methods A and B. Figure 7 shows the spectral estimates for cyclohexane, toluene, DMF, and *n*-heptane using method A, and Figure 8 shows the spectral estimates using method B. Comparison of these two figures shows again the improved signal-to-noise of the spectral estimates obtained when all 1152 Raman spectra are analyzed together. Some spectral artifacts are observed in the weaker Raman scattering solvents. It is known that bands from very strong signals can remain partially imbedded in very weak signals when spectral reconstruction is performed with BTEM.[15] This arises from the inherent limitations and uncertainties associated with weak signals, as well as the experimental design used (low variation in solvent, 150 μL $\pm$ experimental error of each solvent was used in each well).

An unexpected result was obtained using method A. Although silicone vacuum grease was used to seal the multiwell cover to the multiwell plate, transport of solvents from adjacent wells was detectable (it seems that the sealing was not 100% effective). Consequently, for the row of cyclohexane solvent wells adjacent to the toluene solvent wells, some signal intensity from toluene was observed (and

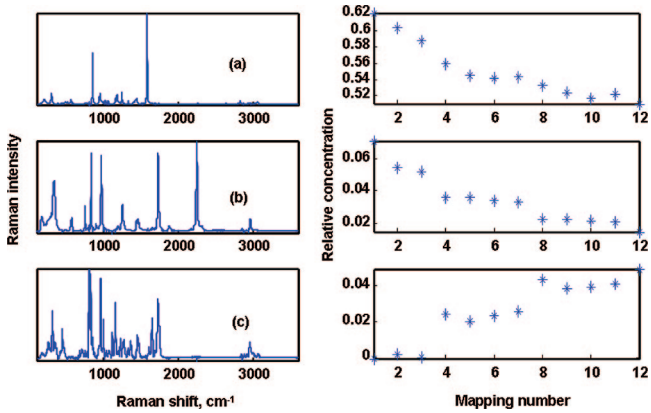

Figure 9. Relative concentration profiles as a function of mapping number. The relative concentrations have been normalized against the solvent intensity. (a) 1,3-Cyclohexadiene, (b) alkyne, and (c) product.

vice versa). The same situation was also observed for the row of toluene solvent wells adjacent to the DMF solvent wells (and vice versa). However, this situation was not observed for the row of *n*-heptane solvent wells adjacent to the DMF solvent wells. Therefore, it appears that gastight sealing was achieved in some situations but not all situations. Although always quite small, the unexpected signals from the transported solvents increased slowly with time. It also can be mentioned that the presence of transported solvents and their increased time dependencies in adjacent wells was conclusively confirmed by full range (100−3600 cm^{-1}) BTEM spectral analysis and least-squares fitting.

Additional tests of the data were performed. In particular, BTEM spectral estimates were mapped back, using least-squares fitting, onto the time-dependent despiked Raman spectra from the individual reaction wells. Wells 15, 18, 21, and 24 were studied in detail. These wells had the same initial concentrations of reagents, but different solvents. The relative concentration profiles for well 15 are shown in Figure 9 after normalization to the solvent intensity. It is clearly seen that the reagent concentrations decrease and that the product concentration increases with time. The apparent step changes at data points 3−4 and 7−8 are not artifacts but are the result of only day-time mappings being acquired.

A comparison between wells 15, 18, 21, and 24 was made using the conversion of alkyne (conversion is a dimensionless number). Figure 10 shows the mapping-number-dependent conversions of alkyne. This figure shows that all solvents are relatively good solvents for the cycloaddition reaction. This is consistent with the rather well-known solvent-insensitivity of this reaction.[26,27]

Discussion and Conclusion

The current results demonstrate that the combined use of Raman microscopy, multicomponent multiwell plate experimental design, and BTEM analysis is a useful tool for high throughput experimentation. The nonreactive results clearly showed that the data sets from multicomponent mixtures are sufficient for good pure component spectral estimation. Moreover, the reactive experiments showed how the analysis of fixed-reaction and multiple solvent experiments can be facilitated by this combined approach. This greatly simplifies

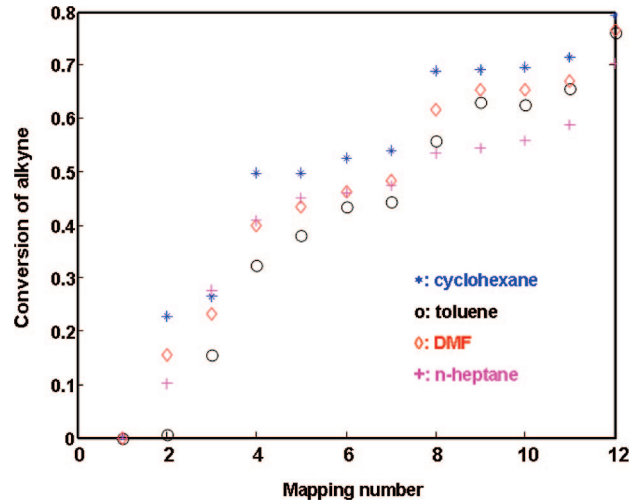

Figure 10. Conversion of alkyne versus the mapping-number for wells 15, 18, 21, and 24 (cyclohexane, toluene, DMF, and *n*-heptane as solvent, respectively). Mapping numbers 1−3 were measured on the 1st day; mapping numbers 4−7 were measured on the 2nd day, and mapping numbers 8−12 were measured on the 3rd day (see Table 1 for details).

analysis because a solvent-by-solvent approach can be avoided. Taken together, the nonreactive and simple reactive experiments demonstrate the considerable usefulness of the BTEM algorithm for combinatorial work and establishes proof of concept for the present approach.

Although the present fixed-reaction and multiple solvent experiment establishes the utility of the main idea (combining Raman microscopy, multiwell plate experimental design, and BTEM analysis), many other frequently asked HTE questions also appear applicable. In addition to solvent optimization, the screening of additional reactants, additional catalysts, additional coadditives, and even different temperatures all appear applicable. Because BTEM has a demonstrated ability to provide dozens of good spectral estimates from well designed experiments[28] and because BTEM can recover good spectral estimates for solutes at trace levels (i.e., ppm or lower[21,22]), the present approach is not restricted to "simple" reactions. Accordingly, combinatorial reactions exhibiting chemo- and regioselectivities can also be investigated (both chemo- and regioselective reactions have been successfully analyzed by BTEM in previous noncombinatorial studies[21−23]). In addition, the present approach appears applicable, at least in principle, to solid-phase syntheses. Since the main aim of the present study was to establish the validity of a combined Raman−multiwell plate−BTEM approach, the present study does not address more complex reaction chemistries.

The present study indicates a few experimental areas requiring further consideration, before more complex reaction chemistries can be effectively studied. These include the desirability of gastight sealing of the multiwell plate, as well as agitation/stirring in each well when surveying reactions. Indeed, good agitation is a prerequisite to high experimental reproducibility. From a software viewpoint, automated and repetitive mapping as a function of time would be useful.

Acknowledgment. This work was supported by the Science and Engineering Research Council of A*STAR (Agency for Science, Technology and Research), Singapore.

References and Notes

(1) Chisholm, B. J.; Webster, D. C. *J. Coat. Technol. Res.* **2007**, *4*, 1–12.
(2) Mishra, K. P.; Ganju, L.; Sairam, M.; Banerjee, P. K.; Sawhney, R. C. *Biomed. Pharmacother.* **2008**, *62*, 94–98.
(3) Fauchere, J. L.; Henlin, J. M.; Boutin, J. A. *Analusis* **1997**, *25*, 97–101.
(4) Bienayme, H.; Schmitt, P. *Actual. Chim.* **2000**, *9*, 29–34.
(5) Keifer, P. A. *Prog. Drug Res.* **2000**, *55*, 137–211.
(6) Anderton, C. *Am. Pharma. Rev.* **2007**, *10*, 36–40.
(7) Mercier, K. A.; Powers, R. *J. Biomol. NMR* **2005**, *31*, 243–258.
(8) Gerrard, D. L. *Anal. Chem.* **1994**, *66*, 547R–57R.
(9) Grossman, W. E. L. *Anal. Chem.* **1976**, *48*, 261R–268R.
(10) Hoettges, K. F.; Huebner, Y.; Broche, L. M.; Ogin, S. L.; Kass, G. E. N.; Hughes, M. P. *Anal. Chem.* **2008**, *80*, 2063–2068.
(11) Kojima, T.; Onoue, S.; Murase, N.; Katoh, F.; Mano, T.; Matsuda, Y. *Pharm. Res.* **2006**, *23*, 806–12.
(12) Kojima, T.; Matsuda, Y. *Pharm. Technol. Japan* **2007**, *23*, 2461–2469.
(13) Widjaja, E.; Li, C. Z.; Garland, M. *Organometallics* **2002**, *21*, 1991–1997.
(14) Chew, W.; Widjaja, E.; Garland, M. *Organometallics* **2002**, *21*, 1982–1990.
(15) Widjaja, E.; Li, C. Z.; Chew, W.; Garland, M. *Anal. Chem.* **2003**, *75*, 4499–4507.
(16) Allian, A. D.; Widjaja, E.; Garland, M. *Dalton Trans.* **2006**, *35*, 4211–4217.
(17) Widjaja, E.; Tan, Y. Y.; Garland, M. *Org. Proc. Res. Dev.* **2007**, *11*, 98–103.
(18) Zhang, H. J.; Garland, M.; Zeng, Y. Z.; Wu, P. *J. Am. Soc. Mass Spectrom.* **2003**, *14*, 1295–1305.
(19) Cheng, S.-Y.; Gao, F.; Krummel, K. I.; Garland, M. *Talanta* **2008**, *74*, 1132–1140.
(20) Guo, L. F.; Wiesmath, A.; Sprenger, P.; Garland, M. *Anal. Chem.* **2005**, *77*, 1655–1662.
(21) Li, C. Z.; Widjaja, E.; Chew, W.; Garland, M. *Angew. Chem., Int. Ed.* **2002**, *41*, 3785–3789.
(22) Li, C. Z.; Widjaja, E.; Garland, M. *J. Am. Chem. Soc.* **2003**, *125*, 5540–5548.
(23) Widjaja, E.; Li, C. Z.; Garland, M. *J. Catal.* **2004**, *223*, 278–289.
(24) Carruthers, W. *Cycloaddition Reactions in Organic Synthesis*; Pergamon Press: New York, 1990.
(25) Safaei-Ghomi, J.; Tajbakhsh, M.; Kazemi-Kania, Z. *Acta Chim. Slov.* **2004**, *51*, 545–550.
(26) Padwa, A. *1,3-Dipolar Cycloaddition Chemistry*; Wiley: New York, 1984.
(27) Huisgen, R.; Fisera, L.; Giera, H.; Sustmann, R. J. *J. Am. Chem. Soc.* **1995**, *117*, 9671–9678.
(28) Chilukoti, S.; Widjaja, E.; Gao, F.; Zhang, H.; Anderson, B. G.; Niemantsverdriet, J. W. H.; Garland, M. *Phys. Chem. Chem. Phys.* **2008**, *10*, 3535–3547.

CC800139X